

Scattering of high-energy phonons at irregular surfaces without and with liquid He

Tsuneyoshi Nakayama*

Department of Engineering Sciences, Hokkaido University, Sapporo 060, Japan

(Received 14 June 1985; revised manuscript received 25 November 1985)

The scattering of high-energy phonons at irregular surfaces without and with liquid He is discussed theoretically by taking account of all eigenmodes of phonons in a solid. It is found that the diffuse component for irregular surfaces without liquid He increases with increasing frequency proportional to ν^4 . The mode-converted surface phonons at irregular surfaces play a role in the diffuse scattering observed in the time-of-flight phonon-reflection experiments. In this connection, the causes of the anomalous behavior of high-energy phonons scattered at the solid-liquid-He interface are discussed. It is pointed out that the mode-converted surface phonons are of considerable importance for the effective phonon transmission across the solid-liquid-He interface. This is concluded from the analysis of the scattering processes of mode-converted surface phonons. The shape of phonon-reflection signals is obtained as a function of time.

I. INTRODUCTION

With the advent of high-energy-phonon generation and detection techniques, it has become possible to study the scattering of phonons of known polarization, frequency, and propagation direction in solids. These techniques have been applied to investigations in various fields of condensed-matter physics.¹ One of the significant applications is the scattering of high-energy phonons at solid surfaces or interfaces. Recently, Taborek and Goodstein²⁻⁴ have succeeded in distinguishing clearly the phonon modes when reflecting at sapphire surfaces with the use of the heat-pulse technique. In addition, they have revealed that bulk phonons (hereafter referred to as B phonons) are scattered both specularly and diffusely at crystal surfaces. An additional striking feature is that diffuse signals are severely affected by placing liquid He at the solid surfaces, but that the specular signals are only slightly influenced. The underlying mechanisms of these phenomena are not yet well understood, though recent studies of the scattering of high-energy phonons with the use of the heat-pulse technique,⁵⁻⁸ phonon imaging,⁹⁻¹¹ and thermal conduction^{12,13} have improved our knowledge of boundary scattering.

The first part of this paper treats the scattering of high-frequency phonons at irregular surfaces *without* liquid He, and clarifies theoretically the cause of the diffuse scattering observed in the time-of-flight phonon-reflection experiments. In the succeeding part, phonon scattering at the solid-liquid-He interface will be discussed. In the present paper the sapphire surface is used for illustration, because sapphire is a mildly anisotropic crystal, which allows one to use the isotropic elastic approximation if the phonon-focusing effect is disregarded. The plan of this paper is as follows: In Sec. II the eigenmodes of phonons in a solid with a free boundary are briefly recapitulated. With the aid of this formalism, the scattering cross sections are obtained for all phonon eigenmodes. Relations between the differential cross sections and the time-of-flight reflection signals are obtained. In

Sec. III it is shown that the diffuse signals are due to two causes. One is direct scattering at irregular surface, B phonon \rightarrow B phonons, and the other is the process B phonons \rightarrow surface phonons (referred to as R phonons), where it is demonstrated that the mode-converted R phonons are backscattered into B phonons by surface irregularities and constitute the diffuse signal. In Sec. IV the shape of the diffuse signal is calculated as a function of time. Section V describes the couplings between phonons and the He system close to the boundary: the displacement-type coupling and the deformation coupling. It is concluded that the *direct* interaction between B phonons and the He system cannot give the effective energy transfer below about 1 THz. In Sec. VI the R-phonon-mediated energy-transfer mechanism is investigated. It is suggested that the mode-converted R phonons play a role in the anomalous absorption of phonons at the solid-liquid-He interface at around 100 GHz. Concluding remarks are given in the final section.

II. MODE CONVERSION OF B PHONONS AT CRYSTAL SURFACE

High-resolution time-of-flight phonon-reflection experiments have revealed that the reflected signals are composed of both specular and diffuse parts.²⁻⁴ The cause of diffuse scattering of the phonons actually lies in the surface irregularities which violate translational invariance parallel to the surface. We could consider various surface irregularities: a rough surface, imperfections like dislocations in the vicinity of the surface, and surfaces covered by chemisorbed or physisorbed impurities. This paper treats mainly the rough surface, since the sapphire surfaces used in the phonon-reflection experiments are known to be well characterized by a scale of roughness of about 100 Å.

There are five phonon eigenmodes specified by J which are orthogonal in the sense of Eq. (A4) (see the Appendix).¹⁴ For the transverse (T) phonons, there exist two kinds of eigenmodes which have a velocity spectrum

$c \geq c_T$, where c_T is the velocity of T phonons. The first mode is the TH mode polarized *parallel* to the surface [see Fig. 1(a)]. The angle θ_H of incidence and reflection is related to c by $\cot^2 \theta_H = \beta^2(c) = (c/c_T)^2 - 1$ and the range of the velocity c is from c_T ($\theta_H = \pi/2$) to infinity ($\theta_H = 0$). The other T mode (referred to as the TV mode) consists of T phonons polarized in the sagittal plane followed by evanescent pseudo-surface-waves [see Fig. 1(b)]. The velocity c of this mode is confined in the finite range $c_T \leq c \leq c_L$, where c_L is the velocity of longitudinal (L) phonons. Another mode consists of mixed longitudinal (L) and transverse (TV) waves with *vertical polarization*, which interact with each other through the surface [Figs. 1(c) and 1(d)]. In these modes c takes a continuous value greater than c_L .

A. Scattering of phonons at rough surfaces

Let us consider a rough surface whose height from the plane $z=0$ is given by a function $f(\mathbf{r})$, where \mathbf{r} is the

two-dimensional position vector. The spatial dependences of the mass density $\rho(\mathbf{x})$ and the elastic constants $\lambda(\mathbf{x}), \mu(\mathbf{x})$ are expressed by combining the roughness function $f(\mathbf{r})$ and the Heaviside step function as $g(\mathbf{x}) = g_0 \Theta(z + f(\mathbf{r}))$,¹⁵ where g_0 is the mean value of the mass density or elastic constants. According to Steg and Klemens,¹⁶ as a first approximation, the bumps of roughness can be described as a mass-density fluctuation. The effects of roughness on the elastic-constant fluctuations are discussed later. For $f(\mathbf{r})$ small compared with the wavelength, as considered here, we can expand the step function as

$$\Theta(z + f(\mathbf{r})) = \Theta(z) - f(\mathbf{r})\delta(z).$$

Thus, one can see that the random part of the mass density is separated as $\Delta\rho(\mathbf{r}) = \rho_0 f(\mathbf{r})$, where $\Delta\rho(\mathbf{r})$ has dimensions of g cm^{-2} . We write the perturbed Hamiltonian due to the mass density fluctuation as^{17,18}

$$H_1 = \sum_{J,J'} (\omega_J \omega_{J'} / 4S^2)^{1/2} \int_0^\infty dz F(\mathbf{k} + \mathbf{k}') \mathbf{u}_J(z) \cdot \mathbf{u}_{J'}(z) \delta(z) [a_J^\dagger(t) - a_J(t)] [a_{J'}^\dagger(t) - a_{J'}(t)], \quad (2.1)$$

where $F(\mathbf{k} + \mathbf{k}')$ is a two-dimensional Fourier transform of the roughness function $f(\mathbf{r})$ and \mathbf{k} is the two-dimensional wave vector [see Eq. (2.3)]. The decay rate of the J -mode phonon into the J' -mode phonon is obtained from the imaginary part of the self-energy given by $\gamma = -2 \text{Im} \langle \Pi(J, \omega_J) \rangle$, and one finds^{17,18}

$$\gamma(J \rightarrow J') = \sum_{\mathbf{k}'} \frac{\pi}{2S} \omega_J^2 \delta(\omega_J - \omega_{J'}) \langle |F(\mathbf{k} + \mathbf{k}')|^2 \rangle \times \left| \int_0^\infty \mathbf{u}_J(z) \cdot \mathbf{u}_{J'}(z) \delta(z) dz \right|^2. \quad (2.2)$$

In Eq. (2.2), the ensemble-averaged Fourier transform of the roughness function is defined by

$$\langle |F(\mathbf{k} + \mathbf{k}')|^2 \rangle = S \int d\mathbf{r} e^{i(\mathbf{k} + \mathbf{k}') \cdot \mathbf{r}} \langle f(\mathbf{r}) f(\mathbf{0}) \rangle, \quad (2.3)$$

where S is the normalization area introduced by integrating over \mathbf{r} .

B. Differential cross section of L phonons

The differential cross section of J -mode phonons is defined by

$$d\sigma(J \rightarrow J') = \frac{\hbar \omega_J \gamma(J \rightarrow J')}{\dot{Q}_J}, \quad (2.4)$$

where \dot{Q}_J is the incident energy flux of J phonons with the velocity c_J given by

$$\dot{Q}_J = \frac{1}{2} \rho_0 |\mathbf{u}_J|^2 \omega^2 c_J S. \quad (2.5)$$

The scattering of T phonons at the solid surface has been

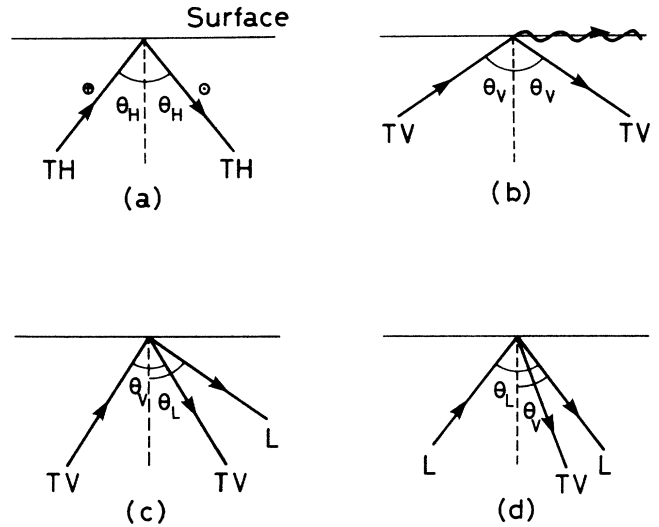


FIG. 1. (a) Transverse mode polarized parallel to the surface. The angle of incidence θ_H is related to $\beta(c)$ by $\cot \theta_H = \beta(c)$, where c takes the continuous values greater than c_T . This mode is denoted as TH mode. (b) Transverse mode polarized in the vertical plane (TV mode). The longitudinal part is localized in the surface. The velocity of the wave front (c) traversing the surface takes the values between c_T and c_L . (c) Transverse mode with vertical polarization (TV mode). The incident TV waves are separated into the transverse and longitudinal waves when reflecting at the surface. The angle of incidence θ_V is obtained through the relation $\cot \theta_V = \delta(c)$ and $c \geq c_L$. (d) Longitudinal (L) mode. The angle of incidence and/or reflection are given by $\cot \theta_L = \delta(c)$ for the L wave and $\cot \theta_V = \beta(c)$ for the transverse wave, where c is greater than c_L .

discussed in a previous short report¹⁹ (hereafter referred to as I). The present paper describes in more detail the problem of the scattering of L phonons. Let us consider the case where L phonons are incident at angle θ_L on a rough surface and are scattered into B phonons. The energy flux of L phonons can be obtained from the first term in square brackets of Eq. (A6) in the Appendix:

$$\dot{Q}_L = \frac{\hbar\omega^2 c}{4\pi c_L \delta(c)}. \quad (2.6)$$

The cross section [Eq. (2.4)] of L phonons into L phonons is obtained as

$$d\sigma(L \rightarrow L) = \frac{W |\zeta'|^2}{c_L^2 c^2 y^4} \left[\frac{\cos^2 \psi}{\delta'} + \delta^2 \delta' \right] dy d\psi, \quad (2.7)$$

where $\zeta = D + iB$ [see Eq. (A7)], $y = c/c_L$, ψ is the angle between the two-dimensional vector \mathbf{k} and \mathbf{k}' , and the factor W is obtained by assuming the white noise for the correlation function (2.3):

$$W = \frac{(\Delta\rho a)^2 \omega^4}{8\pi^2 \rho^2}, \quad (2.8)$$

where a is the characteristic length parameter of the surface roughness. For the process $L \rightarrow TH$, one finds

$$d\sigma(L \rightarrow TH) = \frac{W c_L \sin^2 \psi dx d\psi}{c_T^3 c^2 x^2 \beta'}, \quad (2.9)$$

where $x = c/c_T$. The cross section into TV phonons with spectral range larger than c_L becomes

$$d\sigma(L \rightarrow TV) = \frac{W |\zeta'|^2}{c_L^2 c^2 y^4} \left[\beta' \cos^2 \psi + \frac{\delta^2}{\beta'} \right] dy d\psi, \quad (2.10)$$

and the cross section into TV phonons of spectral range $c_T \leq c \leq c_L$ is obtained as

$$d\sigma(L \rightarrow TV) = \frac{W |A'|^2}{c_L^2 c^2 y^4} \left[\beta' \cos^2 \psi + \frac{\delta^2}{\beta'} \right] dx d\psi. \quad (2.11)$$

In a manner similar to that used in deriving Eqs. (2.7)–(2.11), the cross sections of the reverse processes contributing to the time-of-flight spectra become as follows:

$$d\sigma(TH \rightarrow L) = \frac{W |\zeta'|^2 \sin^2 \psi dy d\psi}{c_T c_L^3 y^4 \delta'}, \quad (2.12)$$

$$d\sigma(TV \rightarrow L) = \frac{W c_T |\zeta'|^2}{c_L^3 c^2 y^4} \left[\frac{\beta^2 \cos^2 \psi}{\delta'} + \delta' \right] dy d\psi, \quad (2.13)$$

and the V mode of the spectral range $c_T \leq c \leq c_L$,

$$d\sigma(TV \rightarrow L) = \frac{W |\zeta'|^2}{c_L^3 c^2 y^4} \left[\frac{\beta^2 \cos^2 \psi}{\delta'} + \delta' \right] dy d\psi. \quad (2.14)$$

C. Decay rate of L phonons into R phonons

Finally, let us consider the rate ($L \rightarrow R$) of L phonons into R phonons. The scalar product in the definition of

$\gamma(L \rightarrow R)$ of Eq. (2.2) yields from Eqs. (A6) and (A9),

$$|\mathbf{u}_L \cdot \mathbf{u}_R|^2 = \frac{kk'}{d\pi K} \left[\frac{\cos^2 \psi f_1^2}{\delta} + \gamma^2 \delta f_2^2 \right], \quad (2.15)$$

where $f_1 = 1 - 2\gamma\eta/(1 + \eta^2)$ and $f_2 = 1 - 2/(1 + \eta^2)$. From Eq. (2.4), one has the cross section

$$d\sigma(L \rightarrow R) = \frac{\pi W c_L}{2c_R^3 c^2 K} (\cos^2 \psi f_1^2 + \gamma^2 \delta^2 f_2^2) d\psi. \quad (2.16)$$

Although the above cross section is not observable directly in the time-of-flight *reflection* experiment, R phonons converted at the rough surface should be rescattered into B phonons by the roughness and constitute the diffuse signal in the time-of-flight experiments. The detailed arguments on the effect of mode-converted R phonons on the time-of-flight reflection experiment are given in Sec. IV.

III. SPECULAR VERSUS DIFFUSE SCATTERING OF TH-PHONONS

In this section we discuss the frequency dependence of the partition ratio between specular and diffuse parts by illustrating TH-mode phonons. The scattering probability of a TH phonon incident at an arbitrary angle θ_H with angular frequency ω into the diffuse scattering part is expressed by

$$t_{\text{dif}} = \hbar\omega \sum_{J' \in \{J_B\}} \Gamma(\text{TH} \rightarrow J') / \dot{Q}_H + \hbar\omega \Gamma(\text{TH} \rightarrow R) / \dot{Q}_H, \quad (3.1)$$

where $\Gamma(\text{TH} \rightarrow J')$ is integrated over the scattered angle:

$$\Gamma(\text{TH} \rightarrow J') = \int \int \gamma(\text{TH} \rightarrow J') dx d\psi$$

and $\{J_B\}$ is the set of all J 's except R phonons. The explicit expression for the first term of Eq. (3.1) is

$$\sum_{J' \in \{J_B\}} \Gamma(\text{TH} \rightarrow J') = \frac{(a\overline{\Delta\rho})^2 \omega^5 c F_1}{(2\pi)^3 (2\rho)^2 c_T^5 \beta}. \quad (3.2)$$

Here the factor $F_1 = I_1 + I_2 + I_3$ is the numerical constant of the value ~ 3.5 , where the first term ($I_1 = \pi$) corresponds to the process $\text{TH} \rightarrow \text{TH}$, and I_2 and I_3 correspond to the decay processes into TV phonons and L phonons. The decay rate of a TH phonon into a R phonon becomes

$$\Gamma(\text{TH} \rightarrow R) = \frac{(a\overline{\Delta\rho})^2 \omega^5 c f_1^2}{4^3 \pi \rho^2 c_T^2 c_R^3 \beta K}. \quad (3.3)$$

Hence, the first term of Eq. (3.1) becomes

$$t_{1M}(\omega, \text{TH} \rightarrow B) = \frac{(a\overline{\Delta\rho})^2 \omega^4 F_1}{8\pi^2 \rho^2 c_T^4}, \quad (3.4)$$

and the second term is obtained as

$$t_{2M}(\omega, \text{TH} \rightarrow R) = \frac{(a\overline{\Delta\rho})^2 \omega^4 f_1^2}{16\rho^2 c_T c_R^3 K}. \quad (3.5)$$

We see from Eq. (3.4) and (3.5) that the component of the

diffuse scattering increases with increasing frequency proportional to the fourth power. This is due to the fact that the correlation function of roughness is taken as the white noise. The extension to the surface which has different correlation characteristics is straightforward, but this is not essential in the present work.

The component of specular reflection coefficient is obtained by extracting the part of the diffuse scattering from unity as

$$r_S = 1 - (t_{1M} + t_{2M}) . \quad (3.6)$$

The sapphire surfaces used in experiments^{2-4,9-10} have a roughness scale of the order of $\delta = 100$ Å. This indicates that one can treat the surface with mean variation in depth and width of $\delta = 100$ Å with the areal density $w = 0.5\delta^{-2}$.¹⁶ The characteristic length δ of roughness should correspond to the length scale a given in Eqs. (3.4) and (3.5), and one can replace $(a\Delta\rho)^2$ by $w(\Delta M)^2$, where the averaged mass of "bump" is estimated as $\Delta M = \rho_0 a^3 = 3.99 \times 10^{-18}$ g for $a = 100$ Å. The resultant probability of the diffuse scattering for TH phonons of frequency ν in GHz yields for sapphire crystal,

$$t_{\text{diff}} \approx 10^{-9} \nu^4 , \quad (3.7)$$

where the following values for sapphire are used: $c_L = 11 \times 10^5$ cm/sec and $c_{\text{TH}} = 6 \times 10^5$ cm/sec. This indicates that TH phonons with frequency around 100 GHz are scattered dominantly into diffuse part and, for sufficient low frequencies ($\ll 100$ GHz), most of the incident phonons are specularly reflected. The same conclusion is true for L phonons. We omit the discussion on this point for L phonons. It should be emphasized that the probability of diffuse scattering t_{diff} cannot exceed unity. From this condition we can estimate the frequency regime where the present analysis is valid. In the case of roughness parameter $\delta = 100$ Å, one has the condition $\nu < 200$ GHz. This value is reasonable because the corresponding wavelength of 200 GHz phonons becomes about 300 Å.

IV. DIFFUSE SIGNALS IN THE TIME-OF-FLIGHT REFLECTION SIGNALS

A. Direct process: B + roughness \rightarrow B

Let us consider the case in which the heater and bolometer are very small and close together. Figure 2 shows the geometry of our system with the definition of the thickness of crystal h and the polar coordinate r . Then each element of the area $dA = r dr d\psi$ on the top surface is irradiated by B phonons emitted from the heater of the Lambertian source and the element dA reradiates phonons. Since the heater and bolometer are assumed to be very small and close together, the bolometer detects only the phonons backscattered with the same angle as that of incident phonons: that is, the element dA can be considered as a new source. Defining $S(t)$ as the heat flux emitted by the heater and taking into account the time delay of arrival at the bolometer $t = 2d/c_J$, where $d = (r^2 + h^2)^{1/2}$, we have the fraction of the reflected intensity

$$dR_1 = \frac{d\sigma(J \rightarrow J', c, \psi) \cos^2 \theta S(t - 2d/c_{JJ'})}{(r^2 + h^2)^2} . \quad (4.1)$$

Here $c_{JJ'}$ is defined as $c_{JJ'} = 2c_J c_{J'} / (c_J + c_{J'})$. The cross section $d\sigma(J \rightarrow J')$ is defined by Eqs. (2.9)–(2.14). The diffuse signal $R_1(t)$ as a function of time is obtained by integrating Eq. (4.1) over r (over the irradiated surface) and assuming the heat pulse described by a δ function

$$S(t) = \delta(t) S_0 . \quad (4.2)$$

This approximation is valid for the crystal of about 1 cm in thickness because heat pulses used in the experiments were of 10–100 nsec duration.²⁻⁶ The relation between r in Eq. (4.1) and x in Eqs. (2.9)–(2.14) is obtained from

$$x^2 = \cot^2 \theta + 1 = (h/r)^2 + 1, \quad x = c/c_J . \quad (4.3)$$

Using this relation, the diffuse signal as a function of time is represented by

$$R_1(t) = S_0 \sum_{J, J' \in \{J_B\}} \int_0^{2\pi} d\psi \int r dr \frac{d\sigma^*(J \rightarrow J') \cos^2 \theta \delta(t - 2d/c_{JJ'})}{(r^2 + h^2)^2} . \quad (4.4)$$

Here the definition of the cross section is

$$d\sigma^*(J \rightarrow J') = d\sigma(J \rightarrow J') / dx d\psi .$$

The resultant expression for L phonons of (4.4) is obtained by defining $R_1 = \sum_i r_i$, where

$$r_1(L \rightarrow L) = \frac{4^3 \pi P W |\xi'|^2}{c_L^{10} t^{12}} \left[\frac{(c_L^2 t^2 / 4 - h^2)^2}{h} + 2h^3 \right], \quad t \geq 2h/c_L , \quad (4.5)$$

$$r_2(L \rightarrow \text{TV}) = \frac{3\pi 4^3 h P W c_T (c_{LT}^2 t^2 / 4 - h^2)}{c_L^5 c_{LT}^6 t^{12}}, \quad t \geq 2h/c_{LT} , \quad (4.6)$$

$$r_3(L \rightarrow \text{TH}) = \frac{4^2 \pi P W c_L (c_{LT}^2 t^2 / 4 - h^2)}{c_T^5 c_{LT}^4 t^{10} h}, \quad t \geq 2h/c_{LT} . \quad (4.7)$$

Here the definition of P is

$$P = \frac{2^5 h^4 S_0}{c_{JJ'}} . \quad (4.8)$$

The other processes concerning T phonons have been given in I.

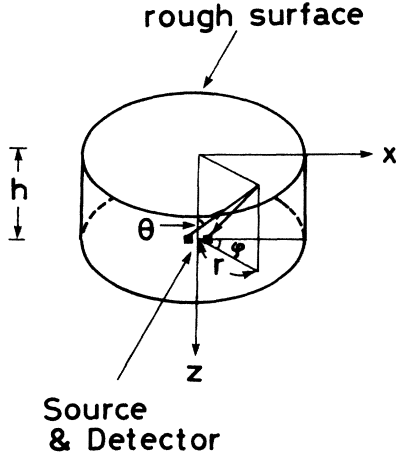


FIG. 2. Geometric arrangement of the present system. The heater and bolometer are assumed to be close together. The crystal thickness is h .

B. Component of R phonons in diffuse signals and its time delay

B phonons scattered at the surface have a high probability of mode conversion into R phonons as shown in the next subsection [see Eq. (4.16)]. At first, to see the effect of mode-converted R phonons on the diffuse signals, let us consider the transition rate of R phonons by roughness. (Note that the mode-converted B phonons at a rough surface are assumed to reach the detector without scattering in the present calculation.) The inverse of the lifetime of R phonons into B' phonons can be obtained by using Eq. (2.2) as well:

$$\Gamma(\text{R} \rightarrow \text{B}) = \frac{2Wf_1^2\omega F_1}{c_T^3 c_R K} \quad (4.9)$$

This transition rate is similar to that obtained by Maradudin and Mills¹⁵ except the numerical factor. For the process (R→R), one has the transition rate,

$$\Gamma(\text{R} \rightarrow \text{R}) = \pi^2 W \omega (f_1 + 2\gamma^4 f_2^4) / (c_R^4 K^2) \quad (4.10)$$

We see, from the ratio of Eqs. (4.9) and (4.10), that the transition rate of R phonons into R phonons is 3.21 times as large as that of R phonons into B phonons: $\Gamma(\text{R} \rightarrow \text{R}) = 3.21\Gamma(\text{R} \rightarrow \text{B})$. It should be noted that Maradudin and Mills¹⁵ obtained the result $\Gamma(\text{R} \rightarrow \text{R}) \simeq 10\Gamma(\text{R} \rightarrow \text{B})$ in their calculation of the attenuation of R phonons due to roughness. In a similar manner done in

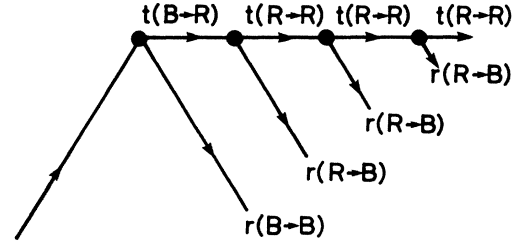


FIG. 3. Higher-order processes of scattering of mode-converted R phonons. The incident energy is normalized to unity; that is, $t(\text{B} \rightarrow \text{R}) + r(\text{B} \rightarrow \text{B}) = 1$.

deriving Eq. (3.4), i.e., replacing the roughness by the defects with the average mass of bumps $\Delta M = \rho_0 a^3$, one finds the effective lifetime of R phonons taking account of Eqs. (4.9) and (4.10),

$$\tau_R \simeq 100\nu^{-5} \text{ sec} \quad (4.11)$$

where ν is in GHz. In deriving Eq. (4.11) the known values for sapphire are used: $c_L = 11.0 \times 10^5 \text{ cm/sec}$, $c_T = 6 \times 10^5 \text{ cm/sec}$, $c_R = 0.92c_{\text{TH}}$, and $\rho_0 = 3.99 \text{ g/cm}^3$. By taking $\nu = 50\text{--}100 \text{ GHz}$, we have $\tau_R \sim 10 \text{ nsec}$. These results indicate that, when R phonons propagate along the rough surface, the R phonons should be backscattered into B phonons with the life time τ_R . This should result in the time delay in the temporal signals of diffuse scattering. However, it is too small to distinguish this time delay in the diffuse signals with our experimental accuracy (since the time duration of heat pulse is 10–100 nsec). Thus, we can neglect the time-delay effect in the analysis of the temporal shape of diffuse tail for the process of mode-converted R phonons.

C. Ratio of intensities of diffuse signals between two processes: B→B and B→R→B

R phonons converted at rough surface should be backscattered into B phonons as mentioned in the previous subsection. This is analyzed in more detail by the following arguments considering the higher-order scattering processes. Let us define the normalized rates of the mode conversion as $r(J \rightarrow J' \neq \text{R})$ for B→B and $t(J \rightarrow \text{R})$ for B→R [see Eqs. (3.4) and (3.5)]. When a J phonon is scattered at rough surface, the incident energy normalized to unity is shared by B phonon and R phonon. This situation is expressed in the following form by considering the higher-order scattering processes (see Fig. 3):

$$r(J \rightarrow J') + t(J \rightarrow \text{R}) \sum_{J' \in \{J_B\}} r(\text{R} \rightarrow J') + t(J \rightarrow \text{R}) \sum_{J' \in \{J_B\}} [1 - r(\text{R} \rightarrow J')] \sum_{J'' \in \{J_B\}} r(\text{R} \rightarrow J'') \\ + t(J \rightarrow \text{R}) [1 - \sum_{J' \in \{J_B\}} r(\text{R} \rightarrow J')]^2 \sum_{J'' \in \{J_B\}} r(\text{R} \rightarrow J'') + \cdots = \sum_{J' \in \{J_B\}} r(J \rightarrow J') + t(J \rightarrow \text{R}) \quad (4.12)$$

Here the first term of the left-hand side is the lowest-order process corresponding to the scattering B→B. The second

term is the second-order process representing the process $B \rightarrow R \rightarrow B$ and the third term indicates the process $B \rightarrow R \rightarrow R \rightarrow B$. One can sum up the left-hand side into the form of the right-hand side of Eq. (4.12) which should become unity from the law of energy conservation. All energy converted from J -mode phonon into R phonon is backscattered into B phonon. Though the more systematic treatment should be made in terms of a Green function, these are not necessary in the analysis of the diffuse signals in the time-of-flight experiments.

Now let us consider the case where J phonons are incident at the rough surface and scattered into the definite $J' \neq R$ phonons and R phonons. These processes are given in the following expression from Eq. (4.11):

$$r(J \rightarrow J') + t(J \rightarrow R)r(R \rightarrow J') + t(J \rightarrow R) \left[1 - \sum_{J' \in \{J_B\}} r(R \rightarrow J') \right] r(R \rightarrow J') + \dots$$

$$= r(J \rightarrow J') + t(J \rightarrow R)r(R \rightarrow J) / \sum_{J' \in \{J_B\}} r(R \rightarrow J'). \quad (4.13)$$

By comparing the first and second term of Eq. (4.13), we have the partition ratio of the processes ($J \rightarrow R$) and ($J \rightarrow J \neq R$),

$$P_{J,J'} = \frac{t(J \rightarrow R)r(R \rightarrow J')}{r(J \rightarrow J') \sum_{J' \in \{J_B\}} r(R \rightarrow J')}. \quad (4.14)$$

For example, the ratio between the processes ($TH \rightarrow TH$) and ($TH \rightarrow R \rightarrow TH$) yields

$$P_{TH,TH} = \frac{t(TH \rightarrow R)r(R \rightarrow TH)}{r(TH \rightarrow TH)[r(R \rightarrow TH) + r(R \rightarrow TM) + r(R \rightarrow L)]}. \quad (4.15)$$

Equation (4.15) is estimated as

$$P_{TH,TH} = \frac{\pi^2 f_1^2}{2K} \left(\frac{c_T}{c_R} \right)^3 (I_1 + I_2 + I_3)^{-1}, \quad (4.16)$$

where $I_1 - I_3$ are defined in Eq. (3.2). Numerical estimation of Eqs. (4.16) is made in the next subsection together with the analysis of the temporal shape of reflection signals.

D. Numerical results

For the calculation of the time-of-flight reflection spectra, the parameters for sapphire are used by identifying the velocity of slow transverse phonons (ST) as that of TH phonons and the fast transverse phonons (FT) as TV phonons; $c_{ST} = 6.0 \times 10^5$ cm/sec, $c_{FT} = 6.5 \times 10^5$ cm/sec, and $c_L = 11.0 \times 10^5$ cm/sec. Figure 4 shows the calculated shape of reflection signals. The thicknesses of crystals are taken to be $h = 1.0$ cm. Curves 6, 5, and 4 correspond to the T phonons $TH \rightarrow TH$, $TH \rightarrow TV$, and $TV \rightarrow TV$. Curves 3, 2, and 1 are due to the L phonons $L \rightarrow TH$, $L \rightarrow TV$, and $L \rightarrow L$. Curve A comes from the mode conversion from B phonons to B phonons, and curve B shows the component of the mode-converted R phonons. The ratio of height of curves 6A and 6B is $p_{TH,TH} = 0.2$ and of 2A and 2B is $p_{TH,TV} = 0.07$. These are calculated from Eq. (4.14). In Fig. 4 we find that curves 2 and 3 are rounded in comparison with the other processes. This indicates the absence of the forward scattering in the processes $L \rightarrow TH$ and $L \rightarrow TV$. This is attributed to the fact that the roughness has been simplified as the mass defects. As seen from the interaction Hamiltonian (2.1), the mass-

defect interaction includes the scalar product of the polarization vectors, and this vanishes for the processes between L phonons and T phonons ($L \rightarrow TH$ and $L \rightarrow TV$). Provided that the fluctuation of the elastic constants are taken into account as done in Ref. 18, one can obtain the sharp peaks for curves 2 and 3.

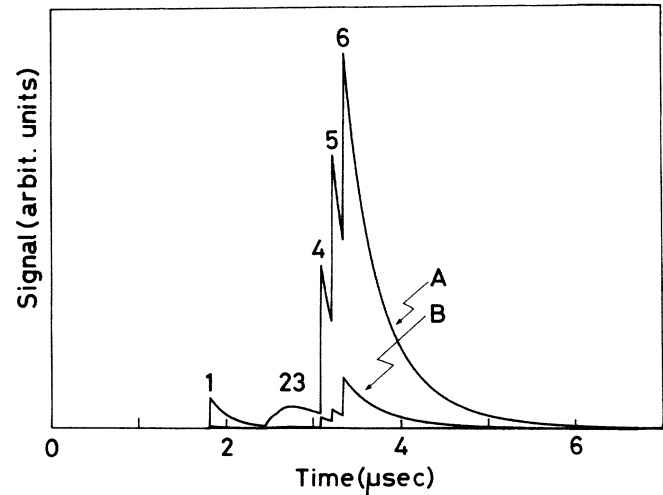


FIG. 4. Calculated results of reflection signal taking into account all phonon modes. Curve A comes from the mode conversion to B phonons. Curve B represents the component of the mode-converted R phonons. The thickness of crystal is taken to be $h = 1$ cm. The peaks (1–6) correspond to the processes $L \rightarrow L$, $L \rightarrow TV$, $L \rightarrow TH$, $TV \rightarrow TV$, $TV \rightarrow TH$, and $TH \rightarrow TH$, respectively.

V. PHONON TRANSMISSION ACROSS THE SOLID-LIQUID He INTERFACE

This and following sections discuss the origin of effective phonon transmission across the solid-liquid He interface. This so-called Kapitza problem above about 1 K has been studied theoretically in two different views:^{20,21} the modification of acoustic mismatch (AM) theory by incorporating surface irregularities, and the quantum mechanical extension taking into account the interaction between phonons and the He system or adsorbed impurities. The modified AM theory yields valuable information with regard to the role of surface irregularities for this problem, but it is unable to provide insight on the striking features observed with the aid of new techniques of phonon generation and detection such as the cosine law of transmitted phonons,²¹ and the isotope effects between ³He and ⁴He.^{22,23} Figures 5(a) and 5(b) are the schematic diagram showing the anomalous transmission of high-energy phonons across the solid-liquid He boundary. A brief outline was published earlier.²⁴ This paper gives the theory in greater detail with various extensions, and brings out clearly the physical significance of the mechanism proposed in the present work.

A. He system close to the boundary

Apart from poorly defined surfaces such as metal surfaces (hard to handle theoretically), one can consider well-characterized surfaces such as those of sapphire used in the phonon reflection experiments.³ It has been well accepted for these cases that the first adsorbed layer of He (next to the surface) is immobile at sufficiently low temperatures with a density similar to that in bulk solid He at a pressure of about 100 atm.²⁵ At the location far from the range of the attractive substrate potential, the liquid He should maintain its bulk properties. The He atoms between the first adsorbed layer and bulk liquid are bound weakly to the substrate and their motion is quite restricted. One can regard it as a dense fluid with no long-range order^{25,26} at temperatures around 1 K, where the most experiments of phonon reflection and transmission have been performed.

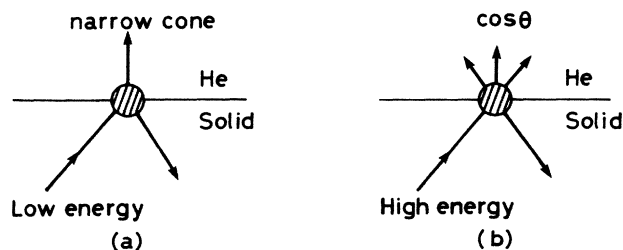


FIG. 5. Schematic diagrams of the scattering of phonons at the solid-liquid-He interface. (a) This shows the scattering of low-energy phonon. The transmitted phonons are within the critical cone determined from the law of momentum conservation. (b) This is the diagram of scattering of high-energy phonons. The angular distribution of transmitted phonons follows the cosine law. The diffuse component of reflected phonons are much influenced in the presence of liquid He.

The two-level tunneling state (TLS) model has been introduced for liquid ³He or ⁴He by Andreev^{27,28} to explain the observed *T*-linear specific heats above the quantum degenerate temperature (no long-range order). The concept of the TLS's for the He system is quite analogous in many respects to the TLS model in glasses originally proposed by Anderson, Halperin, and Varma,²⁹ and Phillips.³⁰ The TLS's are responsible for the universal low-temperature properties shared by all configurationally disordered systems (see Fig. 6). The essential differences of the TLS's between liquid ⁴He (or ³He) and glasses are that He atoms possess high tunneling probabilities due to a large overlap of the wave functions of the He atoms and the density of states per unit energy $n(E)$ of the TLS's is larger than that of glasses by a factor of the order of 10^6 as shown in the later discussion. The TLS model has been also introduced independently by the present author for the He system close to the interface,³¹ where the positions of He atoms should be quite irregularly distributed (no long-range order).

It is interesting to note that the observed specific heats of the adsorbed He system are explainable by the TLS model above a few degrees K both for ³He and ⁴He.³²⁻³⁴ These results are to be compared with those of inelastic neutron scattering on He-layered surfaces revealing dispersionless surface excitations.³⁵ The maximum energy difference E_m can be estimated to be about 100 K from the binding energy of van der Waals potential to the substrate. The magnitude of the level density $\nu(E)$ per one He atom becomes z/E_m , where z is the effective number of neighboring vacant positions. By taking $z \sim 5$ and $E_m \sim 100$ K, the density of states per one atom can be estimated as $\nu(E) = 3 \times 10^{14} \text{ erg}^{-1}$. The number density of He atoms in the first few adsorbed layers is $N \simeq 10^{15} \text{ cm}^{-2}$, so that the density of states per unit area n_0 becomes

$$n_0 \simeq 3 \times 10^{29} \text{ erg}^{-1} \text{ cm}^{-2}. \quad (5.1)$$

This is quite large compared with the density of tunneling states in glasses reduced to per unit area: $n_0 \simeq 10^{25} \text{ erg}^{-1} \text{ cm}^{-2}$.³⁶

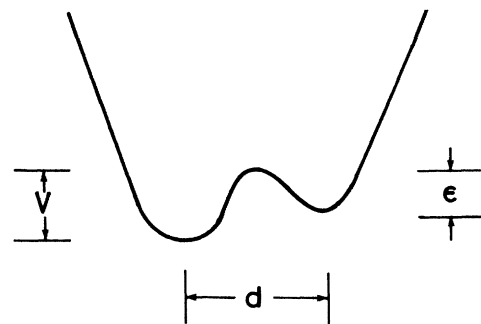


FIG. 6. Double-well potential for He atom or local groups of He atoms close to the solid surface in a configurational space. The potential barrier V and the distance d between wells takes the distribution due to the randomness of the environment of He atoms.

B. Coupling between phonons and He system close to the boundary

An important task in understanding the effective phonon transmission is to determine the type and strength of coupling between phonons and the He system. Under the circumstances that phonons are incident into the the surface in contact with liquid He, the interaction has the effects of scattering and energy absorption. The two types of interaction could be considered for our system. One is the displacement-type coupling and the other the deformation coupling.

1. Displacement-type coupling

Though the displacement-type coupling between adatom and substrate phonons has been studied for many problems since the work of Lennard-Jones and Strachan,³⁷ this coupling needs caution when applying it to our problem, as discussed by Brenig and Schoenhammer.³⁸ They pointed out that, if in the expansion of the substrate-adatom potential V only term linear in the substrate displacement are taken into account, the resulting Hamiltonian does not conserve the total momentum.

Let us consider a TH phonon incident at angle θ to the surface (with parallel polarization to surface) defined through the relation $\cot^2\theta_H = (c/c_H)^2 - 1$ (see Fig. 1). The displacement vector of TH phonons is written as¹⁴

$$\mathbf{u}_{\text{TH}}(\mathbf{x}, t) = \sum_{\mathbf{k}} \left[\frac{\hbar}{2\rho_0\omega_k} \right]^{1/2} (a_{\mathbf{k}} + a_{-\mathbf{k}}^\dagger) \mathbf{u}_{\text{TH}}(z) e^{i(\mathbf{k}\cdot\mathbf{r} - \omega t)}, \quad (5.2)$$

where

$$\begin{aligned} u_x^{\text{TH}}(z) &= -\frac{k_y}{k} \left[\frac{2kc^2}{\pi c_T^2 \beta} \right]^{1/2} \cos(\beta kz), \\ u_z^{\text{TH}}(t) &= 0. \end{aligned} \quad (5.3)$$

Here ρ_0 is the mass density of solid, ω_k the angular frequency, \mathbf{k} the two-dimensional wave vector parallel to the surface, and c is the velocity of the wave front traversing the surface, respectively. a_j and its Hermitian conjugate a_j^\dagger are the annihilation and creation operators of TH mode phonon satisfying the ordinary commutation relation of the Bose type. Following Brenig and Schoenhammer,³⁸ the interaction Hamiltonian can be represented by the quadratic form with respect to the relative displacement between the He atom and the substrate

$$V = \frac{1}{2} f [\mathbf{a} - \mathbf{u}(t)]^2, \quad (5.4)$$

where \mathbf{a} is the coordinates of the He atom measured from the equilibrium position, and f is the coupling constant between the He atom and the substrate. The one-phonon (TH mode) absorption probability (dimensionless) is defined by

$$t_D = \frac{\hbar\omega_d \Gamma_D}{\dot{Q}_{\text{TH}}(\omega_k)}, \quad (5.5)$$

where $\dot{Q}_{\text{TH}}(\omega_k)$ is the incident energy flux defined by Eq.

(2.5) and $\hbar\omega_d$ is the energy difference between the ground state and the first excited state of the He atom bound in the attractive potential from the substrate. The transition rate (sec^{-1}) for the normal incidence of the TH mode phonon Γ_D due to the coupling Eq. (5.4) becomes, using the first-order perturbation theory,

$$\Gamma_D = \frac{N\hbar\omega_d^3}{\rho_0 c_T S} \delta(\hbar\omega_k - \hbar\omega_d), \quad (5.6)$$

where N/S is the number of He atoms per unit area. In deriving Eq. (5.6) we have used the relation $\omega_d^2 = f/m_{\text{He}}$. As a result, one has the one-phonon absorption probability

$$t_D = \frac{2N\hbar\omega_k^2 m_{\text{He}}}{\rho_0 c_T S} \delta(\hbar\omega_k - \hbar\omega_d). \quad (5.7)$$

It should be noted that this absorption probability is expressed by the known physical parameters. We can obtain the same sum rules from Eq. (5.7) with those obtained by Maris.³⁹ The absorption rate of a TH phonon by the TLS with a broad distribution of energy difference can be obtained by replacing the δ function $\delta(\hbar\omega_k - \hbar\omega_d)N/S$ in Eq. (5.7) by n_0 . Taking account of the temperature dependence, one has

$$t_D = \frac{2n_0\hbar\omega_k^2 m_{\text{He}}}{\rho_0 c_T} \tanh(\hbar\omega_k/2k_B T). \quad (5.8)$$

By using the explicit value of n_0 of Eq. (5.1) we have the absorption probability t_D (corresponding to the transmission coefficient) to be

$$t_D \cong 6.9 \times 10^{-8} \nu^2, \quad (5.9)$$

where ν is expressed in GHz. If one considers a phonon of 100 GHz incident at the surface, the rate becomes $t_D = 6.9 \times 10^{-4}$. This is too small to transfer energy effectively in the frequency regime considered here as well as the conclusions of Ref. 39. These calculations are, however, based on the assumption of noninteracting He atoms close to the boundary. When the surface density of adsorbed He atoms becomes high, we need to incorporate the interaction of He atoms. As a result, $\hbar\omega_d$ in Eq. (5.7) is replaced by the smaller value than the value estimated from the van der Waals potential for a single atom.

2. Deformation coupling

The other important interaction arises from the coupling proportional to the strain called deformation coupling. We should bear in mind that the physical natures of He atoms close to the boundary include the contribution from the He atoms and/or substrate surrounding the He atoms. When a TH phonon is incident at the rough surface, the substrate surface atoms are deformed locally by an incident phonon; i.e., the phonon works as a deformation coupling proportional to the strain $e_{\alpha\beta}$. The He atoms close to the surface should change the states by rearranging the atomic configuration quantum mechanically from this coupling. As a consequence, the He system close to the interface has a new energy state E_f , which differs from the initial one E_i . Because the spread of the wave packet of He atoms is small with respect to

the special change of the strain, one can estimate the atomic energy difference as

$$E_f - E_i = \sum_{\alpha, \beta} \frac{\partial E_i}{\partial e_{\alpha\beta}} e_{\alpha\beta}, \quad \alpha, \beta = x, y, z. \quad (5.10)$$

We can estimate the strength of deformation coupling constant $g_{\alpha\beta} = \partial E / \partial e_{\alpha\beta}$ for the TLS from Eq. (5.10) by postulating the complete deformation of $e_{\alpha\beta} = 1$. Due to this deformation the change of the binding energy of the He atom should be of the order of the van der Waals potential so that the deformation coupling constant becomes about $g = 100$ K. Thus, the interaction Hamiltonian between a TH phonon with the wave vector \mathbf{k} and the He system is expressed in the second quantized form,

$$H_k = g_k \eta_k \sigma_x, \quad (5.11)$$

where the operator σ_x is the Pauli matrix. The strain η_k is obtained using the displacement field of a TH phonon of normal incidence as

$$\eta_k = - \left[\frac{\hbar k_z^3}{\rho_0 \omega_k \pi S} \right]^{1/2} \sin(k_z z) (a_k + a_{-k}^\dagger). \quad (5.12)$$

For phonons with much longer wavelength compared with roughness scale δ , the above strain component vanishes at the boundary ($z=0$), of course. For phonons with short wavelength this is not the case, and there is a nonvanishing contribution of the strain component. If the variation of roughness is comparable with the wavelength of an incident TH phonon, it is reasonable to take the average value

$$\langle \sin^2(k_z z) \rangle = \frac{1}{a} \int_0^a \sin^2(k_z z) dz.$$

As a result, the absorption probability due to the above deformation Hamiltonian (5.11) becomes, using Eq. (5.5),

$$t_S = \frac{2\pi g^2 n_0 \omega}{\rho_0 c_T^3} \tanh \left[\frac{\hbar \omega_k}{2k_B T} \right]. \quad (5.13)$$

In deriving Eq. (5.13) we have used the following transition rate calculated by the time-dependent perturbation theory

$$\Gamma_S = \frac{g^2 \omega^2 n_0}{\rho_0 c_T^3} \tanh \left[\frac{\hbar \omega_k}{2k_B T} \right]. \quad (5.14)$$

The density of state per unit area n_0 is estimated in Eq. (5.1). If we take the values for the mass density of a solid and the velocity of a TH phonon for sapphire as $\rho_0 = 3.99$ g cm⁻³, $c_T = 6.0 \times 10^5$ cm sec⁻¹, and $g = 100$ K, the absorption probability for frequency ν in GHz is

$$t_S \simeq 2.56 \times 10^{-6} \nu. \quad (5.15)$$

For the incident phonon of $\nu = 100$ GHz, the absorption probability becomes $t_S \simeq 2.56 \times 10^{-4}$. This is too small to explain the experiments ($\sim 10^{-1}$) as well as the case of the displacement coupling obtained in Eq. (5.9).

Apart from the phonon absorption by the adsorbed He system, there is an interesting possibility that adsorbed air molecules constitute two-level tunneling states similar to

those of glasses.^{39,40} The phonon absorption rate for these cases is obtained as well by using Eq. (5.13) which is the same as that obtained by Kinder.⁴⁰ From the density of states per unit volume obtained for fused silica $n_0 \simeq 10^{33}$ cm⁻³ erg⁻¹, as a typical value, we can estimate the density of states per unit area as

$$n_0 \simeq 10^{25} \text{ cm}^{-2} \text{ erg}^{-1}. \quad (5.16)$$

The deformation coupling constant is known to be of the order of $g \simeq 1$ eV.³⁶ Using these values, we have the scattering rate for frequency ν in GHz as

$$t_G \simeq 1.12 \times 10^{-6} \nu. \quad (5.17)$$

This is also too small to explain the phonon-reflection experiments as well as Eq. (5.15). In this connection it should be mentioned that Shingh *et al.*⁴¹ searched for the existence of TLS similar to glasses in the adsorbed layer of water molecules on small γ -alumina particles with an average diameter of 70 Å. They could not, however, obtain the evidence showing the TLS in these layers.

C. Interaction between phonons in liquid He and two-level systems close to the boundary

Provided that the TLS is excited by absorbing the phonon energy from a solid, it returns to the initial state by emitting a phonon into a solid or liquid. We can conclude from the following arguments that the coupling with phonons in liquid He are very strong compared with that of phonons in a solid so that the excited TLS emits a phonon into liquid He dominantly. The type of coupling between phonons in liquid He and the TLS close to the boundary should be the deformation type.³¹ The expression of the decay rate $\Gamma_{\text{He-L}}$ of the TLS due to the interaction with phonons in liquid He becomes the same form with Eq. (5.14), where the mass density and the velocity of phonons are replaced by those of liquid He. As a result, one has the ratio of the transition rates from Eq. (5.14) as

$$\frac{\Gamma_{\text{He-S}}}{\Gamma_{\text{He-L}}} = \frac{\rho_L v_L^3}{\rho_S c_T^3} \simeq 10^{-4}, \quad (5.18)$$

where the mass density of liquid ⁴He of $\rho_L = 0.145$ g cm⁻³ and the velocity of phonons in liquid ⁴He of $v_L = 2.38 \times 10^{-4}$ cm sec⁻¹ are used. Because the transition rate of the TLS by emitting a phonon into liquid He is as large as that obtained in Eq. (5.18), it is appropriate to consider that all phonon energy absorbed by the He system is emitted into the He system. Thus, it is sufficient to calculate the absorption probability of phonons by the adsorbed He layer using formula (5.5) in order to discuss the origin of phonon transmission across the solid-liquid He interface.

VI. EFFECTIVE ENERGY TRANSFER INTO LIQUID He

In Eqs. (5.9) and (5.15), we have shown that the *direct* interaction process of phonon absorption (B phonons to He system) is negligible. Let us be reminded, however, of the experimental evidences^{3,5-8} that diffusely scattered

phonons play a key role to transfer the energy effectively. In Sec. IV we clarified that diffuse signals are due to two causes. One is the direct scattering of B phonons at irregular surfaces (B phonons + roughness \rightarrow B phonons), and the other due to the mode-converted R phonons (B phonons + roughness \rightarrow R phonons \rightarrow B phonons). Thus, another possibility of the effective energy transfer occurs through the interaction between R phonons and the He system: The R phonons converted from B phonons at rough surface interact with the He system, and the energy of R phonons are absorbed by the He system (see Fig. 7). If the lifetime of mode-converted R phonons due to interaction with the He system (τ_H) is shorter than that of R phonons due to scattering by roughness (τ_R), the phonon energy converted into R phonons should be transferred into the He system. (Note that due to the large acoustic mismatch, the classical leaking of energy of R phonons into liquid He for rough surfaces is small compared with that from the decay of R phonons to the TLS.) As a consequence, the component of R phonons of diffuse signals ($\sim 20\%$) should vanish when liquid He is present (see Fig. 4). Let us compare in the following subsections the lifetimes τ_H and τ_R of R phonons due to the above two scattering processes.

The lifetimes of mode-converted R phonons due to interaction with the He system are obtained from the following two types of interactions.

A. Displacement-type coupling

The lifetime due to the displacement-type interaction between R phonons and the He system is calculated straightforwardly by replacing the surface displacement $u_{\text{TH}}(0)$ in Eq. (5.4) by that of R phonons (A9) as

$$u_z^R(0) = -\gamma \left[\frac{\hbar k}{2\rho_0\omega_k K S} \right]^{1/2} f_2(a_k + a_{-k}^\dagger). \quad (6.1)$$

The inverse of lifetime $\tau_{H,d}$ becomes, from Eq. (6.1),

$$\frac{1}{\tau_{H,d}} = \frac{\pi\hbar\gamma^2 m_{\text{He}}\omega_k^3 f_2^2 n_0}{2\rho_0 K c_R} \tanh \left[\frac{\hbar\omega_k}{2k_B T} \right]. \quad (6.2)$$

Taking the numerical values for sapphire, we have the lifetime of R phonons with frequency in GHz under the condition $\hbar\omega_k > 2k_B T$,

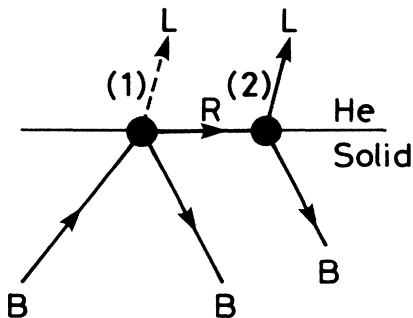


FIG. 7. Two possible channels of energy transfer. Process (1) represents the direct process and (2) represents the R phonon mediated process of energy transfer.

$$\tau_{H,d} \simeq 0.88 \times 10^{-2} \nu^{-3} \text{ sec}. \quad (6.3)$$

B. Deformation coupling

The lifetime of R phonons due to the deformation interaction can be obtained by using Eq. (5.11) and the wave function of R phonons as

$$\frac{1}{\tau_{H,s}} = \frac{\pi n_0 \omega_k^2 g^2}{\rho_0 c_L^3 K} \tanh \left[\frac{\hbar\omega_k}{2k_B T} \right]. \quad (6.4)$$

It should be noted that the frequency dependence of Eq. (6.4) is different from that of bulk phonons $\sim \omega_k$.³⁶ This comes from the fact that the energy density of R phonons is localized in the vicinity of the surface of order of its wavelength; i.e., the energy density is frequency dependent. The numerical estimation of Eq. (6.4) for frequency ν in GHz for sapphire gives

$$\tau_{H,s} \simeq 1.02 \times 10^{-3} \nu^{-2} \text{ sec}. \quad (6.5)$$

The ratio of lifetimes of R phonons due to scattering by roughness and the TLS is obtained from Eqs. (4.11) and (6.3) as

$$\tau_{H,d} / \tau_R \simeq 10^{-4} \nu^2 \quad (6.6)$$

from the displacement-type coupling. For the deformation coupling one has the ratio from Eqs. (4.11) and (6.5) as

$$\tau_{H,s} / \tau_R \simeq 10^{-5} \nu^3. \quad (6.7)$$

From Eqs. (6.6) and (6.7) we see that the mode-converted R phonons are absorbed effectively by the He system for the frequency about 100 GHz. Note that if the influence of surface irregularities to the density of states of TLS is taken into account, we should have a much shorter lifetime than the estimation of Eqs. (6.3) and (6.4). As a consequence, the diffuse tail arising from the mode-converted R phonons vanishes when the surface is in contact with liquid He at around 100 GHz of phonon energy; i.e., the diffuse signal to the mode-converted R phonons (curve B in Fig. 4) vanishes. These are the reasonable results for explaining the anomalous phonon scattering at the liquid-He–solid interface.

VII. CONCLUDING REMARKS

The scattering of high-frequency phonons at irregular surfaces without and with liquid He has been discussed theoretically by taking into account all phonon eigenmodes in a solid with a free boundary. We have calculated the frequency dependence of the partition ratio between the diffuse and specular component for the surface without liquid He, and obtained that the diffuse component is proportional to the fourth power of frequency. The shapes of phonon reflection spectra have been calculated as a function of time. The role of mode-converted R phonons to the diffuse signals in a time-of-flight spectra has been discussed in detail by considering the higher-order scattering processes of the mode-converted R phonons. It has been shown that there exist six processes of

the mode-conversion when reflected at the rough surface. The additional important conclusion is that the diffuse signals are composed of two causes: One comes from the direct scattering (B phonons \rightarrow B phonons), and the second is due to the R phonon mediated scattering process (B \rightarrow R \rightarrow B, B \rightarrow R \rightarrow R \rightarrow B, and so on). The mode-converted R phonons are of considerable importance in the interpreting of the origin of the diffuse scattering of high-frequency phonons as seen from Fig. 4.

It has been experimentally revealed that the diffuse signals are strongly influenced by placing liquid He at the solid surface.^{3,5-8} In this connection, the mode-converted R phonons should play an important role for the effective energy transfer into liquid He, as concluded from the comparison of lifetimes of R phonons due to the surface roughness and the interaction with the He system. Of the characteristic features observed by the transmission or reflection experiments, we need the consistent theoretical explanation of the following experimental findings: The cosine law of transmitted phonons into liquid He,⁴² the importance of the surface irregularities,⁴³ the role of diffusely scattered phonons for phonon transmission,^{3,5-8} and the presence of an "energy gap" for phonon absorption.^{22,44-46}

At low frequencies it is well accepted that the classical channel obeying the AM theory is restricted by the critical cone. By increasing frequency, the angular-distribution measurements show that there is another channel for conductance which carries most of the energy. The shape of the anomalous channel is not restricted by the critical one and radiates phonons into all directions.⁴² In the present mechanism this cosine law of transmission follows from an isotropic distribution of two-level tunneling states. The cosine law does not result in the surface irregularities. Considerable theoretical effort has been expended in an attempt to elucidate how surface irregularities perform their role for the energy transfer.^{47,48} The present mechanism is different from these in many respects. The anomalous energy transfer is observed even for the surfaces in contact with solid ³He and ⁴He.^{46,49} These surfaces are exposed to air and would be covered by a few adsorbed air molecules in which He atoms can be embedded. For these dirty surfaces, He atoms close to the interface should be randomly distributed due to the misfitting of atomic configuration between the substrate atoms and He atoms. Thus, it is expected that, for the dirty surface, the TLS's are composed of both He atoms and disordered layer.

We have treated the problem as simply as possible in order to clarify the underlying the mechanism of the problem. The isotropic elastic approximation is used for a solid. Solids are generally anisotropic in an elastic property which results in the focusing effect of the phonon propagation as discussed in detail by Taborek and Goodstein.³ For the detailed comparison with experiments it is necessary to consider the anisotropic nature of crystals. This is an interesting future theoretical problem. The formula determining the ratio of diffuse and specular scattering, Eq. (3.1), is valid under the condition $t < 1$. This scattering probability t is proportional to the roughness scale δ^4 , namely, sensitive to the substrate characteristics. Crystal surfaces covered by a few adsorbed air molecules possess a

possibility that this layer constitutes the highly attenuating layer³⁹ for high-energy phonons. Especially, if the wavelength of incident B phonons is comparable with the thickness of these dirt layers, these layers should affect the interaction between B phonons and the He system.

In conclusion, the results presented here will be useful for resolving the unsettled problem of anomalous phonon transmission across the solid-liquid-He surface. After completing this manuscript, the author found the experimental works^{50,51} concerning the present subject. Burger *et al.*⁵¹ have observed only specular reflection and no He effect for low-energy phonons. For high-energy phonons a big change of the diffusely scattered component was found when the Si surface was in contact with liquid He. These results seem to be explainable from the mechanism discussed in the present work.

ACKNOWLEDGMENT

This work was supported in part by a Grant-In-Aid from the Ministry of Education, Sciences and Culture, Japan.

APPENDIX: PHONONS IN A SOLID WITH FREE BOUNDARY

Provided that an isotropic elastic continuum occupies the half space $z \geq 0$ with a stress-free boundary at $z = 0$, the displacement vector at a point $\mathbf{x} = (\mathbf{r}, z)$ and time t can be expanded in terms of eigenmodes¹⁴

$$\mathbf{u}(\mathbf{x}, t) = \sum_J \left[\frac{\hbar}{2\rho\omega_J} \right]^{1/2} [a_J(t) + a_J^\dagger(t)] \mathbf{u}_J(\mathbf{x}), \quad (\text{A1})$$

where ρ is the mass density of a solid, $J = (\mathbf{k}, c, m)$ represents a set of quantum numbers which specifies the eigenmodes of phonons, c is the velocity of a wave front traversing the surface, and m specifies the mode. The sum over J is defined as

$$\sum_J = \frac{1}{(2\pi)^2} \int d\mathbf{k} \left[\sum_{m \neq R} \int_{D_m} \frac{dc}{c} f(\mathbf{k}, c, m) + f(\mathbf{k}, c_R, R) \right], \quad (\text{A2})$$

where D_m denotes the spectral range of the velocity c for the mode m , and \mathbf{k} is the two-dimensional wave vector parallel to the surface. R represents the Rayleigh mode (representative surface mode) whose amplitude decreases exponentially with the distance from the surface. In Eq. (A1) a_J and a_J^\dagger are an annihilation and creation operator of the J -mode phonon satisfying the following commutation relation:

$$[a_J, a_{J'}^\dagger] = \delta_{J, J'}. \quad (\text{A3})$$

Here the symbolic expression $\delta_{J,J'}$ should be understood to be

$$\delta_{J,J'} = \delta_{m,m'} \delta_{\mathbf{k},\mathbf{k}'} \delta_{c,c'} . \quad (\text{A4})$$

If c and c' belong to continuous spectra (B phonons), we use the definition $\delta_{c,c'} = c\delta(c - c')$. The \mathbf{r} dependence of $\mathbf{u}_J(\mathbf{x})$ is described by a plane wave originating from the translational invariance parallel to the surface:

$$\mathbf{u}_J(\mathbf{x}) = \mathbf{u}_J(z) e^{i\mathbf{k}\cdot\mathbf{r}} / S^{1/2} , \quad (\text{A5})$$

where S is the surface area and $\mathbf{u}_J(z)$ represents the amplitude of J phonons along the depth from the surface.

The L phonons are reflected at a surface into both L phonons and TV phonons as a result of the interaction with each other through the surface [see Figs. 1(c) and 1(d)]. The wave function of L modes are constructed from the linear combination of the mixed L-TV mode as obtained by Ezawa.¹⁴ The explicit form of the wave function of the mode depicted in Fig. 1(c) becomes

$$u_{j=x,y}^{\text{LT}}(z) = -\frac{k_j}{k} \left[\frac{k}{2\pi} \right]^{1/2} [\delta^{-1/2}(e^{-i\delta kz} - De^{i\delta kz}) + \beta^{1/2} Be^{i\beta kz}] , \quad (\text{A6})$$

$$u_z^{\text{LT}}(z) = \left[\frac{k}{2\pi} \right]^{1/2} [\delta^{1/2}(e^{-i\delta kz} + De^{i\delta kz}) + \beta^{-1/2} Be^{i\beta kz}] ,$$

where

$$\delta(c) = [(c/c_L)^2 - 1]^{1/2}, \quad \beta(c) = [(c/c_T)^2 - 1]^{1/2}, \quad (\text{A7})$$

$$D = \frac{(\beta^2 - 1)^2 - 4\alpha\beta}{(\beta^2 - 1)^2 + 4\alpha\beta}, \quad B = \frac{4(\alpha\beta)^{1/2}(\beta^2 - 1)}{(\beta^2 - 1) + 4\delta\beta} .$$

The first two terms in the square brackets of Eq. (A6) represent L waves, and the third term means TV waves. The factor D has the physical meaning of the reflection coefficient of L phonons at a surface. The angle of incidence and/or reflection is defined by the relation $\cot\theta_L = \delta(c)$.

For the modes shown in Fig. 1(d) we have

$$u_{j=x,y}^{\text{TL}}(z) = i \frac{k_j}{k} \left[\frac{k_j}{2\pi} \right]^{1/2} [\delta^{-1/2} Be^{i\delta kz} + \beta^{1/2}(e^{-i\beta kz} + De^{i\beta kz})] , \quad (\text{A8})$$

$$u_z^{\text{TL}}(z) = i \left[\frac{k}{2\pi} \right]^{1/2} [\delta^{1/2} Be^{i\delta kz} + \beta^{-1/2}(e^{-i\beta kz} - De^{i\beta kz})] ,$$

where the first term represents the L waves and the last two are the TV waves, in which D represents also the reflection coefficient of TV waves at a solid surface. The angle of incidence and/or reflection is obtained from the relation $\cot\theta_V = \beta(c)$. In the above two modes [Eqs. (A6)–(A8)], c takes the continuous value greater than c_L .

The wave function of R phonons is expressed as

$$u_{j=x,y}^{\text{R}}(z) = i \frac{k_j}{k} \left[\frac{k}{K} \right]^{1/2} \left[e^{-\gamma kz} - \frac{2\gamma\eta}{1+\eta^2} e^{-\eta kz} \right] , \quad (\text{A9})$$

$$u_z^{\text{R}}(z) = -\gamma \left[\frac{k}{K} \right]^{1/2} \left[e^{-\gamma kz} - \frac{2}{1+\eta^2} e^{-\eta kz} \right] .$$

Here, $\gamma^2 = [1 - (c_R/c_T)^2]$, $\eta^2 = [1 - (c_R/c_L)^2]$, and $K = (\gamma - \eta)(\gamma - \eta + 2\gamma\eta^2)/2$, where c_R is the velocity of R-mode phonon.

*Present address: Department of Applied Physics, Faculty of Engineering, Hokkaido University, Sapporo 060, Japan.

¹For instance, see the review in *Non-equilibrium Phonon Dynamics*, NATO Advanced Study Institute Series B, edited by W. Bron, (Plenum, New York, 1985).

²P. Taborek and D. Goodstein, *J. Phys. C* **12**, 4737 (1979).

³P. Taborek and D. Goodstein, *Phys. Rev. B* **22**, 1550 (1980).

⁴P. Taborek and D. Goodstein, *Solid State Commun.* **33**, 1191 (1980).

⁵D. Marx and W. Eisenmenger, *Z. Phys. B* **48**, 277 (1982).

⁶D. Marx and W. Eisenmenger, *Phys. Lett.* **93A**, 152 (1983).

⁷J. T. Folinbee and J. P. Harrison, *J. Low Temp. Phys.* **32**, 469 (1978).

⁸H. C. Basso, W. Dietsche, H. Kinder, and P. Leiderer, in *Pho-*

non Scattering in Condensed Matter, edited by W. Eisenmenger, K. Lassmann, and S. Doettinger (Springer-Verlag, Heidelberg, 1984) p. 212.

⁹G. L. Koos, A. G. Every, G. A. Northrop, and J. P. Wolfe, *Phys. Rev. Lett.* **51**, 276 (1983).

¹⁰A. G. Every, G. L. Koos, and J. P. Wolfe, *Phys. Rev. B* **29**, 2190 (1984).

¹¹G. A. Northrop and J. P. Wolfe, *Phys. Rev. Lett.* **52**, 2156 (1984).

¹²L. J. Challis, A. A. Ghazi, and M. N. Wybourne, *Phys. Rev. Lett.* **48**, 756 (1982).

¹³R. O. Pohl and B. Stritzker, *Phys. Rev. B* **25**, 3608 (1982).

¹⁴H. Ezawa, *Ann. Phys. (N.Y.)* **67**, 438 (1971).

¹⁵A. A. Maradudin and D. L. Mills, *Ann. Phys. (N.Y.)* **100**, 262

- (1976).
- ¹⁶R. G. Steg and P. G. Klemens, *Phys. Rev. Lett.* **24**, 381 (1970).
- ¹⁷T. Nakayama and T. Sakuma, *J. Appl. Phys.* **47**, 2263 (1976).
- ¹⁸M. Narita, T. Sakuma, and T. Nakayama, *J. Appl. Phys.* **49**, 5507 (1978).
- ¹⁹T. Nakayama, *Phys. Rev. B* **32**, 777 (1985).
- ²⁰A. C. Anderson, in *Phonon Scattering in Solids*, edited by L. J. Challis, V. W. Rampton, and A. F. G. Wyatt (Plenum, New York, 1976), p. 1.
- ²¹A. F. G. Wyatt, in *Nonequilibrium Superconductivity, Phonons, and Kapitza Boundaries*, NATO Advanced Study Institute Series B, edited by K. E. Gray, (Plenum, New York, 1981), Vol. 65, p. 31.
- ²²O. Koblinger, U. Heim, M. Welte, and W. Eisenmenger, *Phys. Rev. Lett.* **51**, 284 (1983).
- ²³O. Koblinger, E. Dittrich, U. Heim, M. Welte, and W. Eisenmenger, in *Phonon Scattering in Condensed Matter*, edited by W. Eisenmenger, K. Lassmann, and S. Doettinger (Springer-Verlag, Heidelberg, 1984), p. 209.
- ²⁴T. Nakayama, *J. Phys. C* **18**, L667 (1985).
- ²⁵D. F. Brewer, A. J. Symonds, and A. L. Thomson, *Phys. Rev. Lett.* **15**, 182 (1965).
- ²⁶B. C. Crooker, B. Hebrall, E. N. Smith, Y. Takano, and J. D. Reppy, *Phys. Rev. Lett.* **51**, 666 (1983).
- ²⁷A. F. Andreev, *Pis'ma Zh. Eksp. Teor. Fiz.* **28**, 603 (1978) [*JETP Lett.* **28**, 556 (1978)].
- ²⁸A. F. Andreev and Yu. A. Kosevich, *Zh. Eksp. Teor. Fiz.* **77**, 2518 (1979) [*Sov. Phys.—JETP* **50**, 1218 (1979)].
- ²⁹P. W. Anderson, B. I. Halperin, and M. Varma, *Philos. Mag.* **25**, 1 (1972).
- ³⁰W. A. Phillips, *J. Low Temp. Phys.* **7**, 351 (1972).
- ³¹T. Nakayama, *J. Phys. C* **10**, 3274 (1977).
- ³²D. W. Princehouse, *J. Low Temp. Phys.* **7**, 287 (1972).
- ³³D. C. Hickernell, E. O. Mclean, and O. F. Vilches, *J. Low Temp. Phys.* **13**, 241 (1973).
- ³⁴J. G. Daunt and P. Mahadev, *Physica* **69**, 562 (1973).
- ³⁵H. J. Lauter, H. Godfrin, C. Tiky, H. Wiechert, P. E. Obermayer, *Surf. Sci.* **125**, 265 (1983).
- ³⁶See the review by S. Hunklinger and W. Arnold, *Physical Acoustics* (Academic, New York, 1976) Vol. 12, p. 155.
- ³⁷T. E. Lennard-Jones and C. Strachen, *Proc. R. Soc. London, Ser. A* **5**, 442 (1935).
- ³⁸W. Brenig and K. Schoenhammer, *Z. Phys. B* **34**, 283 (1979).
- ³⁹H. J. Maris, *Phys. Rev. B* **19**, 1443 (1979).
- ⁴⁰H. Kinder, *Physica* **107B**, 549 (1981).
- ⁴¹G. P. Shingh, M. von Schickfus, S. Hunklinger, and K. Dransfeld, *Solid State Commun.* **9**, 951 (1981).
- ⁴²R. A. Sherlock, N. G. Mills, and A. F. G. Wyatt, *J. Phys. C* **8**, 300 (1975).
- ⁴³J. Weber, W. Sandmann, W. Dietsche, and H. Kinder, *Phys. Rev. Lett.* **40**, 1469 (1978).
- ⁴⁴E. S. Sabisky and C. H. Anderson, *Solid State Commun.* **17**, 1095 (1975).
- ⁴⁵A. C. Anderson and W. L. Johnson, *J. Low Temp. Phys.* **7**, 1 (1972).
- ⁴⁶J. T. Folinsbee and A. C. Anderson, *Phys. Rev. Lett.* **31**, 1580 (1973).
- ⁴⁷N. S. Shiren, *Phys. Rev. Lett.* **47**, 1466 (1981).
- ⁴⁸J. C. A. van der Sluijs and M. J. van der Sluijs, *J. Low Temp. Phys.* **44**, 223 (1981).
- ⁴⁹J. S. Buechner and H. J. Maris, *Phys. Rev. Lett.* **34**, 316 (1975).
- ⁵⁰H. Kinder, A. De Ninno, D. Goodstien, G. Paterno, F. Scaramuzi, and S. Cunsolo, *Phys. Rev. Lett.* **55**, 2441 (1985).
- ⁵¹S. Burger, K. Lassmann, and W. Eisenmenger, *J. Low Temp. Phys.* **61**, 401 (1985).